Effects of dehydration and grinding on the mechanical shear behaviour of Ca-rich montmorillonite

F. Dellisanti[a], A. Calafato[a], G.A. Pini[b], D. Moro[a,c], G. Ulian[a,c], G. Valdrè[a,c,*]

[a] Dipartimento di Scienze Biologiche, Geologiche e Ambientali, Università di Bologna "Alma Mater Studiorum", Piazza di Porta San Donato 1, 40126 Bologna, Italy
[b] Dipartimento di Matematica e Geoscienze, Università degli Studi di Trieste, via Weiss 2, 34128 Trieste, Italy
[c] Centro di Ricerche Interdisciplinari di Biomineralogia, Cristallografia e Biomateriali, Università di Bologna "Alma Mater Studiorum", Piazza di Porta San Donato 1, 40126 Bologna, Italy

ARTICLE INFO

Keywords:
Ca-rich montmorillonite
Mechanical shear test
XRD
SEM
Mechanical modelling

ABSTRACT

In order to investigate in detail the effects of dehydration and grinding on the mechanical shear behaviour of Ca-rich montmorillonite, a cycle of specific experimental shear deformation tests were performed on five typology of samples, preliminary controlled by thermal analysis (TG, DTA) and X-ray diffraction (XRD): (1) a natural Ca-montmorillonite containing about 5% of adsorbed water; (2) the same montmorillonite heated at 80 °C for 2 h to remove only the adsorbed water; (3) up to 250 °C for 2 h to remove also the interlayer water; (4) up to 340 °C for 2 h to complete the removal of interlayer water and start to introduce thermo-structural defects, and (5) the starting natural Ca-rich montmorillonite after hard ball-milling for 20 h to induce mechanical deformation and structural defects in the TOT layers. The five typologies of samples have been tested by a specifically designed and built shear box apparatus, under about 20 MPa condition of normal pressure. All samples, before and after the shear test, have been analysed by Optical Microscopy (OM), Scanning Electron Microscopy (SEM) and XRD. A theoretical mechanical analysis based on the Maxwell model is proposed to explain the $\tau(\varepsilon)$ and $\tau(\dot{\varepsilon})$ shear behaviour of the effects of the different type of dehydration and deformation of the material, that was finally discussed in the context of the microstructural OM, SEM and XRD data.

1. Introduction

Many works have shown that the mechanical behaviour of soils is influenced by the content of clay fraction and the type of clay minerals, and that a change in shearing mechanism can occur based on the arrangement of clay particles (Skinner, 1969; Vaughan et al., 1976; Hight et al., 1979; Lupini et al., 1981). As a general approach, a reduction of residual friction angle was noted in concomitance to the increase of clay content (Skempton, 1964; Chandler, 1984) both in non-cohesive soil without preferential orientation of particles and in pure clay, in which an alignment of clay platelets occurs along the principal failure surface (Morgenstern and Tchalenko, 1967; Yong and McKyes, 1971). Olson (1974) has performed various shear tests on pure minerals (kaolinite, illite and montmorillonite) to delineate the relationship between the mechanical properties and the kind of clay mineral, and thus drawing a dependence of shear strength from interaction of the particles and the different structural arrangement of clay minerals.

However, the fine relationships between clay dehydration and grinding on the mechanical shear behaviour of clay minerals have never been investigated in detail. It was only shown that a decrease of structural ordering and an increase of lattice defects of smectite can involve changes in the most important physical properties, such as cation exchange capacity (Christidis et al., 2004, 2005; Filipović-Petrović et al., 2002), swelling index (Volzone et al., 1987; Novak et al., 1982; Dellisanti and Valdrè, 2005) and particle size distribution (Christidis et al., 2004, 2005; Dellisanti and Valdrè, 2005). In addition, the possible influence of mechanical grinding and related destabilization of the montmorillonite TOT structure on the mechanical shear behaviour of montmorillonite still need to be investigated.

The scope of the present work is to investigate the details of the relationships between dehydration and grinding on the shear behaviour of montmorillonite. In particular, a cycle of specific experimental shear tests was performed on well-characterized natural Ca-rich montmorillonite samples. To this aim, five typologies of samples were considered and controlled by thermal analysis (TG, DTA) and X-Ray powder Diffraction:

(1) a natural Ca-montmorillonite containing about 5% of adsorbed water;
(2) the same montmorillonite heated at 80 °C for 2 h to remove only the

* Corresponding author.
E-mail address: giovanni.valdre@unibo.it (G. Valdrè).

Accepted 14 November 2017

adsorbed water;
(3) up to 250 °C for 2 h to remove also the interlayer water;
(4) up to 340 °C for 2 h to complete the removal of the interlayer water;
(5) the starting natural Ca-rich montmorillonite after hard ball-milling for 20 h to induce mechanical deformation and structural defects in the TOT layers, but still containing all types of water molecules.

Montmorillonite was used because presents two important types of water molecules: (i) adsorbed water on the surface, and (ii) interlayer water molecules. Furthermore, to investigate and compare the effect of mechanical deformation (defective TOT structure, but still containing water molecules) on the shear behaviour of montmorillonite, some starting natural samples were hard ball milled and successively shear tested without removing any type of water molecules.

Before and after the shear deformation, all the samples have been also analysed from both morphological (optical microscope and SEM observations) and structural points of view (X-ray diffraction).

Finally, a theoretical mechanical analysis, based on the Maxwell's model, is proposed to explain the $\tau(\varepsilon)$ and $\tau(\dot{\varepsilon})$ shear behaviour of the effects of the different type of dehydration and deformation of the montmorillonite, with a related discussion considering the macro- and microstructural OM, SEM and XRD data.

The presented approach and the related results may find great usefulness not only in soil science and geotechnics, but also in practical and industrial applications of clay minerals, in particular montmorillonites and other swelling, non-swelling and deformed, grinded phyllosilicates. Indeed, montmorillonites are commonly used materials for the production of composites for several applications, such as fuel cells (Wu et al., 2016), polymeric (semi) conductors (Bandara et al., 2005), photocatalysis (Menesi et al., 2008). The results here presented could be helpful, for example, in applications where montmorillonite is employed as lubricant material (Cao et al., 2017; Dong et al., 2015), where the knowledge of the shear mechanical behaviour is of utmost importance.

2. Materials and analytical methods

2.1. Materials and thermal analysis control

The sample used in the present work is a powdered montmorillonite sample, of about 25 μm average grain size, provided by Laviosa SpA (Livorno, Italy). It is mainly composed by Ca-montmorillonite (content > 95%) and opal CT and feldspars as minor phases. The ball-milled grinded sample is represented by this natural commercial Ca-montmorillonite that was mechanically deformed for 20 h *via* a planetary ball mill (Pulverisette 5, Fritsch, Germany), as described by Dellisanti and Valdrè (2005). This mechanical treatment induced a partial destruction of crystalline lattice and an increase of structural disorder in the TOT layers of the montmorillonite, still maintaining all types of water molecules in the sample (adsorbed and interlayer).

In order to plan the thermal treatments to the montmorillonite to specifically remove the different types of water molecules, the thermo-structural behaviour of the natural Ca-montmorillonite – cross checked by X-ray Powder Diffraction (*vide infra*) – was previously studied with a Setaram Labsys double furnace apparatus with simultaneous recording of thermogravimetric (TG) and differential thermal analysis (DTA) data. Thermal analysis was performed in the range 20 to 800 °C with a heating rate of 10 °C/min, using about 60 mg of material/sample, platinum crucibles, calcined Al_2O_3 as reference substance, a flow rate of helium of 0.27 ml/s. The temperature accuracy was about ± 1 °C.

2.2. X-ray diffraction and scanning electron microscopy

All the typology of montmorillonite samples were analysed by powder X-Ray Diffraction (XRD): (i) the starting montmorillonite (not sheared), (ii) the thermal treated not sheared montmorillonites and finally (iii) the thermal treated sheared montmorillonites. Analyses were performed by using a Philips PW 1710 diffractometer equipped with a graphite monochromator on the diffracted beam, using CuKα radiation, 40 kV/30 mA power supply, 1° divergence and detector slits, 0.02° (2θ step size and a counting time of 10 s/step. XRD patterns were collected from 3° to 65° (2θ). A quasi-random specimen preparation was used as a reference for the natural, heated and ball-milled samples. X-ray diffraction patterns were evaluated using the Winfit computer program (Krumm, 1996), which allows to decompose the spectra and to obtain the crystallographic parameters of (001) and (060) diffraction peaks of montmorillonite. The selected reflections are important mineralogical parameters for Ca-montmorillonite, as the (001) peak can be related to the distance between TOT layers, and consequently on the presence of water molecules in the interlayer, whereas the (060) peak relates to di-trioctahedral character.

Morphology, fabric and alignment of particles of both sheared and not sheared samples were observed by using first an optical microscope, and successively a scanning electron microscope SEM (JSM-5400 JEOL) working at 10 kV of electron accelerating voltage and with a beam current of about 1 nA at the specimen level. Samples were gold-coated with a layer about 10 nm thick with a vacuum of 0.13 Pa metal-coating process.

2.3. Specifically designed shear box apparatus

Direct shear $\tau(\varepsilon)$ tests on soil and mineral specimens are usually carried out in the Casagrande's box (Casagrande, 1932), where samples of 60 × 60 × 20 mm are subjected to a pressure of about 1 MPa. To increase the normal stress up to about 20 MPa, to simulate a pressure behaviour in technological and lithostatic applications, a modified Casagrande's box apparatus was developed and employed, which presents a reduced specimen size surface (from 36 cm^2 to 5 cm^2) (see Fig. 1). The chosen surface area is the result of a compromise between having a higher confining pressure and analysing a specimen not too small with respect to the scale of structures forming during the shear deformation, the latter to make the edge effects negligible.

All the $\tau(\varepsilon)$ tests were performed at room temperature (about 25 °C) and humidity of about 50–60%. The specimens were tested without adding of water. Initially, the powder was pressed in the specimen cell, and loaded with a constant normal stress of about 20 MPa for 140 h. After this time interval, all the samples reached a stable condition under the imposed normal loading, that is there were no significant deformations by compaction. A relatively high rate of shear deformation ($\dot{\varepsilon}$), starting from about $2.16 \times 10^{-4}\ s^{-1}$, was imposed because the absence of water does not involve fluids overpressure, thus the measured stresses are expressed in effective value (Terzaghi, 1936).

The maximum and residual shear strength parameters (angle of inner friction and cohesion) of each group of samples were evaluated performing three shear tests in different normal stress conditions (14.7, 19.6 and 24.5 MPa) and using the well-known Mohr-Coulomb model.

2.4. Mechanical modelling

In order to analytically describe the observed stress (τ) *vs* strain (ε) data, we considered the typical approach of non-linear viscoelasticity, using a Maxwell model in the form of

$$\tau = \eta\dot{\varepsilon}[1 - \exp(t/\lambda)] \quad (1)$$

where η is the viscosity of the material, $\dot{\varepsilon}$ is the strain rate, t is the time and λ is the relaxation time. For $t/\lambda \ll 1$, the exponential term (viscous one) has negligible effects and the system can be depicted as a Hookean spring, $\tau \sim G_0\varepsilon$, with G_0 the maximum shear modulus. It is possible to

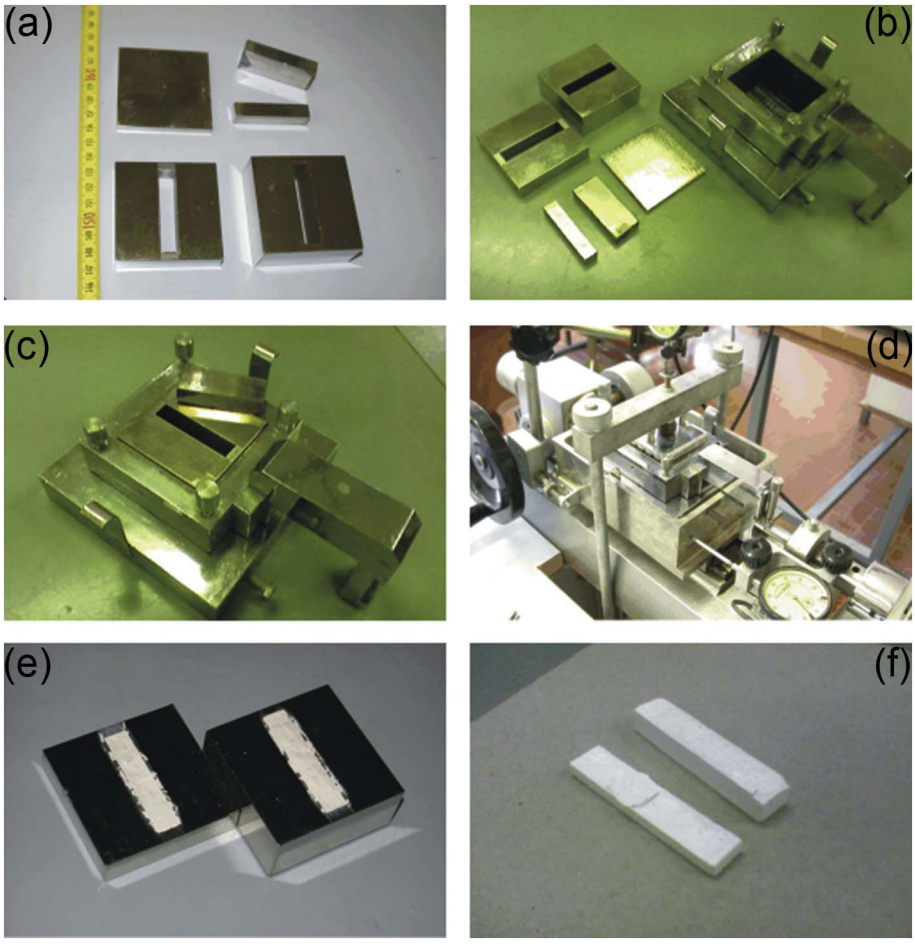

Fig. 1. Shear test apparatus used during the experiments. (a) Auxiliary shear box, (b) main and auxiliary boxes, (c) auxiliary box inserted in the main box, (d) shear test in execution, (e) sample after shear test and (f) sample removed from the auxiliary box.

express the normalized stress response in terms of the transient shear viscosity, which expression is

$$\eta_0^+(t) = \tau^{ideal}(t)/\dot{\varepsilon} = G_0 t \tag{2}$$

Eventually $\eta_0{}^+(t)$ reaches a plateau given by $G_0\lambda$, which is the so called zero-shear viscosity. However, for $t/\lambda > 1$ the damping effect of the viscous term of Eq. (1) leads the stress to a plateau value. In the case of strain softening, at a certain time, the shear stress does not vary according to the previous equation. Beyond $t/\lambda > 1$, the montmorillonite layers start sliding and the elastic plateau modulus $G(\varepsilon)$ is reduced from the equilibrium value G_0 and Eq. (2) becomes generalized:

$$\eta^+(t) = \tau(t)/\dot{\varepsilon} = \eta_0^+(t)h(\varepsilon) \tag{3}$$

where h is the strain softening function, given by

$$h(\varepsilon) = G(\varepsilon)/G_0 \tag{4}$$

3. Results

3.1. Thermal analysis of natural montmorillonite

Results of the thermal analysis (TG, DTA) of the natural Ca-montmorillonite in the temperature range 20–800 °C are reported in Fig. 2. The thermal behaviour is in agreement with previous analysis conducted on similar commercial Ca-montmorillonite samples from Laviosa SpA, and already described in detail by (Dellisanti et al., 2006). The thermal processes occurring by heating the sample can be summarised as:

i) Loss of the water adsorbed on the surface, which is released up to 100 °C;
ii) Loss of interlayer water in the temperature range 100–250 °C;
iii) Simultaneous loss of water from both montmorillonite and the minor components (opal CT) between 250 °C and 700 °C;
iv) Loss of structural hydroxyl groups from the montmorillonite in the range 350–700 °C.

In order to design the shear test on the well-characterized dehydrated montmorillonite samples, thermal analysis data of the starting Ca-montmorillonite were cross-checked to XRD (see Section 3.3). According on previous thermal analyses on smectites (Dellisanti et al., 2006), it was decided to test the following materials by the specifically built shear test apparatus:

1) the starting natural Ca-montmorillonite containing an amount of adsorbed water of about 5%;
2) the natural Ca-montmorillonite after a thermal treatment of 2 h at

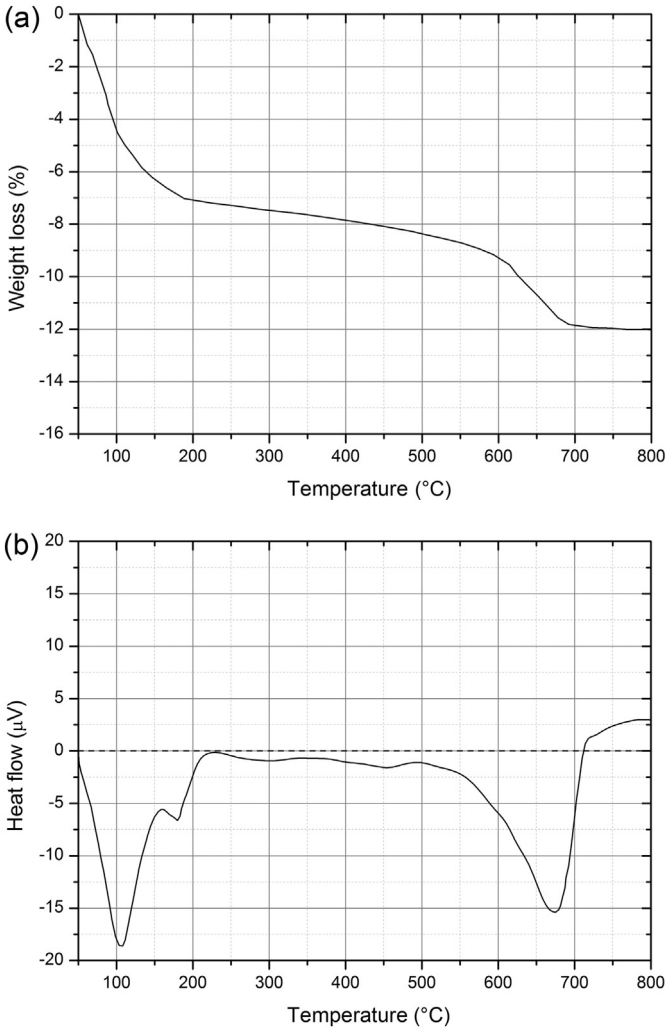

Fig. 2. Thermogravimetric (a) and differential thermal analysis (b) curves obtained for the natural montmorillonite sample.

80 °C to remove the adsorbed water and do not affect the interlayer one that onsets at about 100 °C;

3) the natural Ca-montmorillonite after a thermal treatment of 2 h at 250 °C to remove mainly the interlayer water, even if not completely (see XRD section);
4) the natural Ca-montmorillonite after a thermal treatment of 2 h at 340 °C to be sure to complete the removal of the interlayer water;
5) the ball milled (20 h) natural Ca-montmorillonite containing all type of water molecules to see only the effect of TOT structural deformation during the shear test.

3.2. Morphological characteristics of the shear tested montmorillonite samples

3.2.1. Starting natural montmorillonite

A scaly cleavage related to the interlacing of striated and polished shear planes developed in all the samples of natural Ca-rich montmorillonite along the displacement plane imposed by the experimental apparatus (hereafter defined as principal shear surface, or PSS) (Fig. 3a). Shear planes also cut across part of the specimen far from the PSS. The shear planes are arranged in different oriented sets, disposed at low angle with respect to the PSS as already described by Skempton (1966) and Tchalencko (1968, 1970). The disposition of planes and the lustrous aspect of the surfaces are quite similar to those observed in natural samples (Pini, 1999; Vannucchi et al., 2003; Dellisanti, 2004; Dellisanti and Valdrè, 2005), in clay cake experiments, direct shear (shear box) experiments, triaxial experiments and evidenced by computer simulation (Ahlgren, 2001). Significant features of the clay mineral platelets disposition (fabric) have been pointed out along and in the proximity of shear planes, in which an increase of parallel orientation of the clay platelets occurred. In the SEM analysis of the natural montmorillonite sample, it is possible to observe the clay platelets orientation along the PSS. From the plane view of the shear surface (Fig. 4a) the cited clean striations can be seen, together with several steps due to the compaction and stratifications of the clay platelets. By observing the PSS in a side view, *i.e.* a cross-section of the sample near the shear surface (Fig. 4b), the compaction of montmorillonite after the shear test is more evident, and suggests a decrease of the porosity and relative disposition of the clay platelets as "face-face" arrangement (see for instance Bennet et al., 1981, 1991). Despite, the side view of the sample far from the PSS (Fig. 4c) showed the platelets placed in an "edge-face" disposition (Bennet et al., 1981, 1991) due to a more disordered arrangement of the montmorillonite clay particles. A quite similar fabric is associated to scaly cleavage in natural examples of sheared clays in fault zones (Dellisanti et al., 2008).

3.2.2. Heat treated montmorillonites

Shear deformations of heated samples induced different morphological characters in relation to the presence of adsorption, and/or interlayer water.

The behaviour of montmorillonite heated up to 80 °C for 2 h was quite similar to that of the natural sample, with development of shear planes, but the material is less compacted and the PSS and shear planes are striated but not polished (Fig. 3b). The samples heated up to 250 °C for 2 h did not show striated and polished principal shear surface, as well as there was not both compaction and development of scaly cleavage within specimens (Fig. 3c). The SEM analysis on the sheared sample heated up to 250 °C (Fig. 4d) confirmed the macroscopic observations, showing a lack of compaction that can be noted from the SEM figure, suggesting that the porosity of the sample was not reduced as observed for the sheared natural sample (Fig. 4a). Analogously to the 250 °C samples, in the samples heated up to 340 °C development of striated and polished shear planes and compaction of materials did not occur (Fig. 3d).

3.2.3. Ball-milled grinded montmorillonite

In the ball-milled, grinded defective samples, shear planes were not observed and the specimens appeared not compacted after the shear deformation (Fig. 3e), whereas rare striations can be observed on the principal shear surface. The SEM analysis of these samples (Fig. 4e,f) showed that there is not a re-arrangement of clay particles, and an "edge-face" disposition of the platelets is recognizable. In addition, it can be observed that the disordered clay particles mean size is smaller than the one of non-grinded samples, which is a consequence of the ball-milling process. One of the rare striated areas on the PSS is also reported in the right side of Fig. 4e.

3.3. XRD structural results

XRD analyses were conducted with the same experimental setup and environmental conditions for each sample in order to better compare the different treatments (thermal and mechanical). The intensities in Fig. 5 are relative to the (001) and (060) diffraction peaks, which are the ones mainly affected by the thermal/mechanical treatments, and were reported for each diffractogram as I/I_{max} as a function of 2θ, using CuKα radiation to better compare and cross-correlate the diffraction results. Table 1 reports the calculated relative intensities I/I_{max} and the full widths at half maximum (FWHM) of the (001) and (060) peaks for each sample.

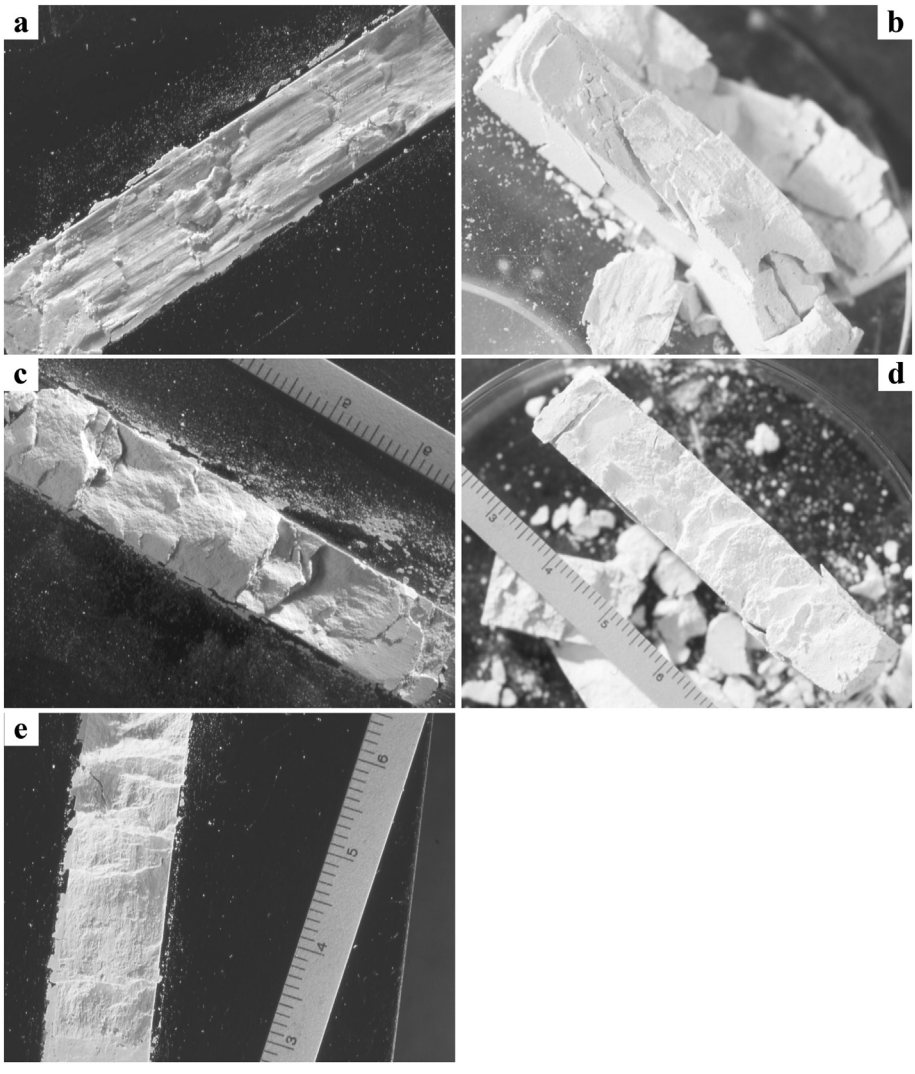

Fig. 3. Morphological characteristics after shear deformation. (a) Detail of polished and striated shear surface in natural Ca-montmorillonite; (b) development of shear planes of montmorillonite heated up to 80 °C; (c) Ca-montmorillonite heated up to 250 °C; (d) Ca-montmorillonite heated up to 340 °C; (e) view of principal shear surface of grinded, defective montmorillonite.

3.3.1. Natural montmorillonite

XRD analysis of the natural starting montmorillonite (Fig. 5a) showed that the intensity of (001) basal diffraction peaks increased in shear deformed samples (at the PSS surface), with a very slight increase of the full width at half maximum (FWHM). Data relative to the (060) diffraction peak show only a decrease of intensity in sheared samples (Fig. 5b), whereas there are no significant changes in FWHM parameters (Table 1).

The above results indicated that the experiments performed by the shear box apparatus induced visible changes in the arrangement of the montmorillonite clay platelets, in agreement with the SEM observations.

3.3.2. Heated montmorillonites

An alignment of clay platelets along shear planes was also shown in the samples heated up to 80 °C and 250 °C, much less evident respect to the natural samples (Fig. 5c,e). Worth to be noted that the sample heated at 250 °C still presents some interlayer water, demonstrated by the 001 diffraction peak at about 6° (2θ), that become more intense after the shear test. Obviously, the (001) angular position of the 250 °C-treated sample is at higher angles of 2θ respect that of the natural montmorillonite, because of the partial loss of interlayer water. Generally, no great changes were observed in the intensity and FWHM of the (060) peaks (Table 1).

On the contrary, the sample heated up to 340 °C did not exhibit an increase of XRD intensity of the (001) peak (Fig. 5g), and in agreement any alignment of particles was not observed by SEM. This sample, as expected, did not show any peak at 6° (2θ), because all the Ca-montmorillonite thermally collapsed to a 10 Å TOT structure, with a broad peak at about 9° (2θ). However, this peak did not increase in intensity after the shear deformation. Also for this sample, generally no great change was observed in the intensity and FWHM of the (060) peaks (see Table 1).

3.3.3. Ball milled grinded montmorillonites

According to the results of Dellisanti and Valdrè (2005), the ball-milled montmorillonite sample presents a broadened, less intense (001) XRD peak respect the natural, not ball-milled sample (Fig. 5i and Table 1). Worth to be noted that the (001) diffraction peak of the ball milled sample is at about 6° (2θ), that demonstrates the presence of interlayer water (Table 1). The mechanical shear test produced, along the principal shear surface, a negligible variation of XRD intensity of the (001) peak respect to the starting ball-milled sample (Fig. 5i). FWHM values remained essentially unchanged. This defective montmorillonite did not show any alignment, suggesting that the clay platelets have generally lost the possibility of a re-arrangement along the principal shear surface, as observed and evinced by SEM analysis, apart in very small areas (Fig. 4e,f). Data related to the (060) peak confirmed a decrease of intensity, indicating an influence of shear strain also in the direction perpendicular to the applied strain (Fig. 5j).

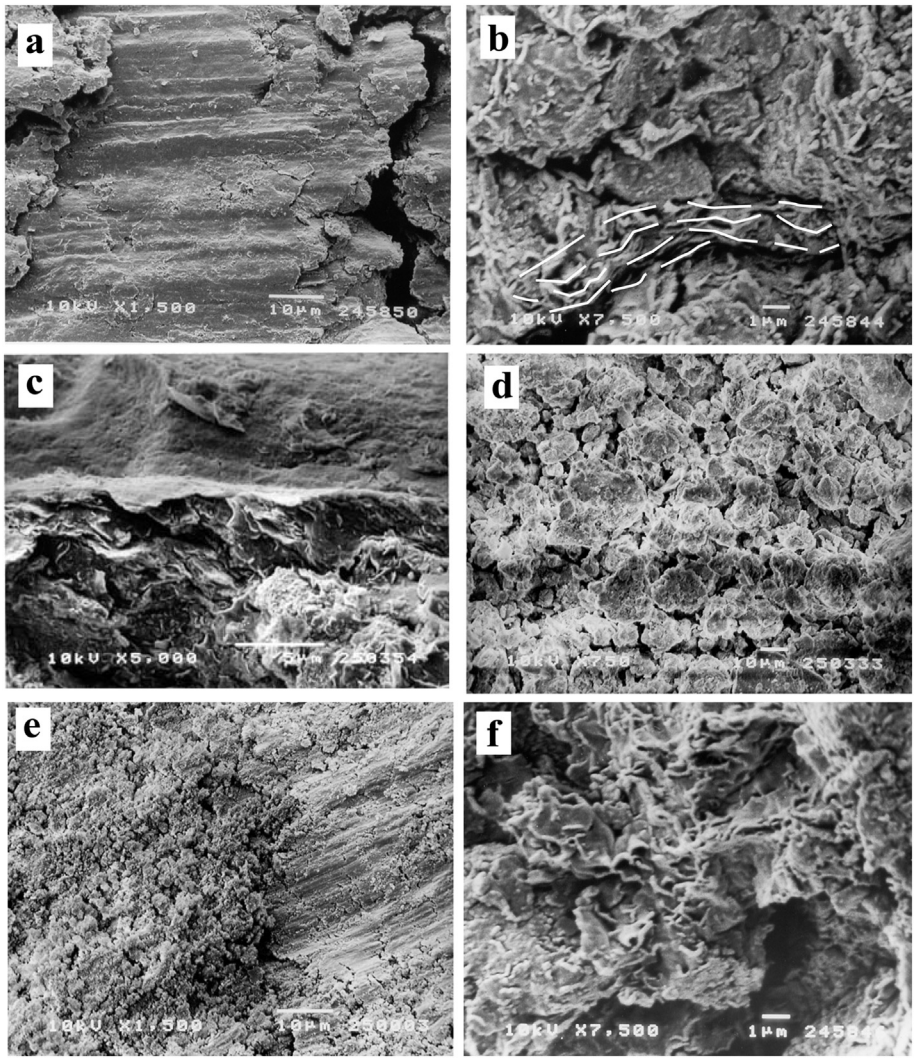

Fig. 4. SEM images of smectite after shear deformation. (a – c) natural Ca-montmorillonite: (a) striated principal shear surface (PSS); (b) alignment of clay platelets along PSS direction (face to face disposition) and (c) disordered arrangement of clay particles far from the PSS of sheared sample (edge to face disposition). (d) Principal shear surface of Ca-montmorillonite heated up to 250 °C. (e, f) Defective Ca-montmorillonite: (e) principal shear surface of grinded montmorillonite and (f) disordered arrangement of clay particles in the sheared sample (edge to face disposition).

3.4. Shear test mechanical behaviour

The mechanical behaviour of the experimental shear test of the five groups of samples was extremely different as shown by the shear stress *vs* strain τ (ε) and *vs* strain rate τ ($\dot{\varepsilon}$) curves reported in Fig. 6.

The natural Ca-montmorillonite presents the typical $\tau(\varepsilon)$ strain softening behaviour of overconsolidated clayey rocks (Skempton, 1970) at least under the present experimental conditions. The deformation of the montmorillonite has a linear increase up to the maximum shear stress value of the material at about 8 MPa, after this value the failure takes place and the stress rapidly decreases to achieve a minimum value of shear strength at about 6.4 MPa, which is maintained nearly constant for the residual part of the deformation (Fig. 6a). The last part of the curve represents the residual strength developed by the shear surface in almost constant volume conditions with the proceedings of the shear deformation. At the maximum value of shear strength the natural starting sample shows an internal friction angle value φ_p of 17.8° and a cohesion c_p of 1.83 MPa, whilst at the residual shear strength conditions, the friction angle (φ_r) and cohesion values (c_r) are respectively 15.6° and 0.63 MPa (Table 2).

In the sample heated up to 80 °C the cohesion is absent and the material exhibits a $\tau(\varepsilon)$ strain softening behaviour with a higher shear strength values than the natural montmorillonite, and a lower fall of peak strength (Fig. 6a, Table 2).

The samples heated up to 250 °C showed a $\tau(\varepsilon)$ strain hardening behaviour (Fig. 6a) similar to that described by Skempton (1970), with the shear stress increasing rapidly and continuously up to achieve the stress value of about 8 MPa. After this value, the stress of heated samples showed a quasi-plastic deformation. At the maximum value of shear strength, there was no cohesion and the angle of inner friction was 26.7°. Samples heated up to 340 °C did not show cohesion and the mechanical behaviour was quasi-plastic (Fig. 6a, b) (Skempton, 1970).

Finally, the ball-milled grinded (defective) montmorillonite displayed a $\tau(\varepsilon)$ behaviour very similar to the montmorillonite heated up to 340 °C (Fig. 6b). At the maximum of shear strength, the angle of inner friction φ_p is 27.7°.

The data fitted using the Maxwell model (Fig. 6c) showed an increased viscosity of the Ca-montmorillonite as a function of the treatment temperature, with values ranging from 1580(6) MPa s (natural sample) to 2250(6) MPa s (sample heated at 340 °C). The ball-milled natural sample presented a viscosity value of 2235(6) MPa s, which is very close to the one obtained by heating montmorillonite at 340 °C, and in agreement with the stress/strain behaviour (Fig. 6b). In the case of the starting natural Ca-montmorillonite, the strain softening function decreased from unity, where $G(\varepsilon) = G_0$, to a constant value of about 0.8. Heating the natural sample up to 80 °C for 2 h produced a constantly decreasing softening function $h(\varepsilon)$ that reached, at maximum strain, a value of about 0.9. Further increase in temperature resulted in softening functions always very close to unity.

Other information about the mechanical shear behaviour of the Ca-montmorillonite can be obtained by the shear stress *vs* strain rate $\tau(\dot{\varepsilon})$ curves reported in Fig. 6d. In general, all of the tested samples exhibited

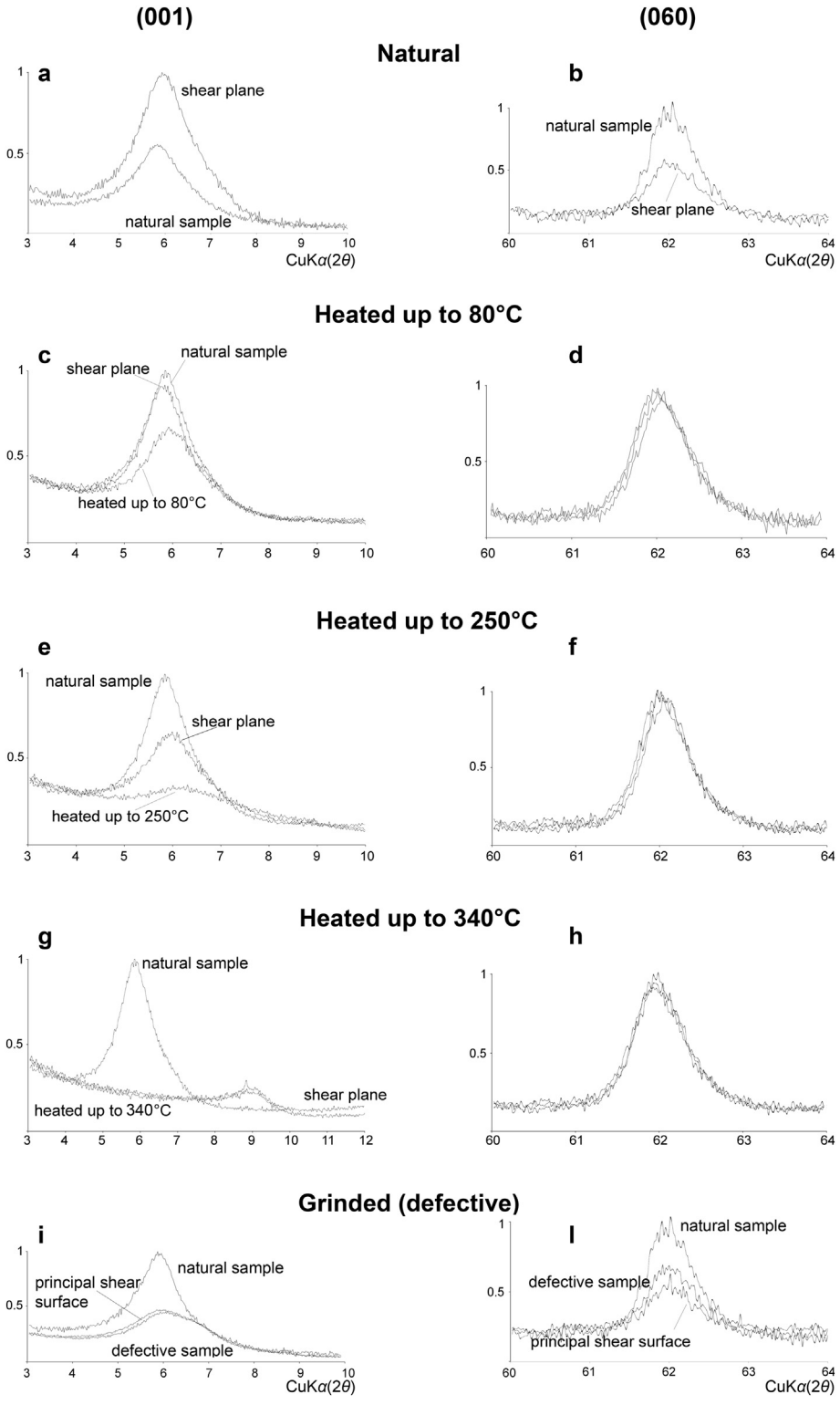

Fig. 5. Comparison between XRD pattern before and after shear test. a,b) (001) and (060) peaks of natural montmorillonite; c, d) (001) and (060) montmorillonite heated up to 80 °C; e, f) (001) and (060) montmorillonite heated up to 250 °C; g, h) (001) and (060) montmorillonite heated up to 340 °C; i, l) (001) and (060) peaks of grinded (defective) montmorillonite. Diffractograms of natural and heated montmorillonite, before and after shear test in (d,f,h) are superimposed.

a behaviour similar to a Bingham plastic material, as the shear rate does not increases until a limit value of the shear stress (yield stress). Our data showed that the yield stress of Ca-montmorillonite reduces as a function of the heating temperature from about 5.1 MPa to 3.2 MPa. However, there is a great difference after the yield point, as untreated (natural) Ca-montmorillonite showed an almost pseudo-plastic behaviour (lowering of the slope of the curve, *i.e.* plastic viscosity), whereas thermally treaded samples resulted, as a function of temperature, in an always more plastic behaviour, showing increased plastic viscosity. The sample heated up to 340 °C, very interestingly, presented a behaviour very similar to that of the deformed (ball milled) sample.

4. Discussion and conclusive remarks

This research introduced new insights on the effects of dehydration and grinding on the mechanical shear behaviour of Ca-montmorillonite.

Macroscopical and microscopical features and the mechanical behaviour of five groups of Ca-montmorillonite samples (natural, heated

Table 1
Comparison of XRD 2θ values (Cu Kα radiation), relative intensity I/I_{max} and FWHM of (001) and (060) diffraction peaks of natural, heated and defective (grinded) montmorillonites. The data were obtained using the software Winfit (Krumm, 1996).

Sample	(001)			(060)		
	Peak angle [°2θ]	I/Imax	FWHM [°2θ]	Peak angle [°2θ]	I/Imax	FWHM [°2θ]
Natural	5.86	0.55	1.10	62.00	1.00	0.62
Sheared	5.96	1.00	1.28	62.02	0.56	0.67
Heated up to 80 °C						
Starting natural	5.85	1.00	0.97	61.99	1.00	0.72
Heated	5.96	0.67	1.13	62.03	0.97	0.69
Heated + sheared	5.82	0.91	1.09	62.06	0.93	0.78
Heated up to 250 °C						
Starting natural	5.85	1.00	0.97	61.99	0.94	0.72
Heated	6.14	0.34	1.93	62.04	1.00	0.73
Heated + sheared	6.00	0.65	1.19	62.06	0.95	0.70
Heated up to 340 °C						
Starting natural	5.85	1.00	1.01	61.99	1.00	0.72
Heated	8.96	0.23	1.22	61.99	0.99	0.80
Heated + sheared	8.96	0.25	1.16	61.97	0.95	0.82
Grinded (defective)						
Starting natural	5.90	1.00	1.08	61.99	1.00	0.64
Grinded	6.10	0.45	1.72	62.00	0.67	0.71
Grinded + sheared	6.06	0.47	1.80	62.00	0.54	0.72

and grinded) appeared significantly different after experimental $\tau(\varepsilon)$ shear test. The shear planes development, the polished and striated surfaces are usually attributed to different structural and grain size characteristics. In particular, a strain softening behaviour is related to the higher phyllosilicates and/or clay minerals content (Skempton, 1964, 1970; Chandler, 1984; Müller-Vonmoos and Honold, 1985; Müller and Schlüchter, 2001).

The present study that deals with samples essentially identical from the mineralogical and granulometric points of view, shows that the significantly different mechanical shear behaviour of Ca-

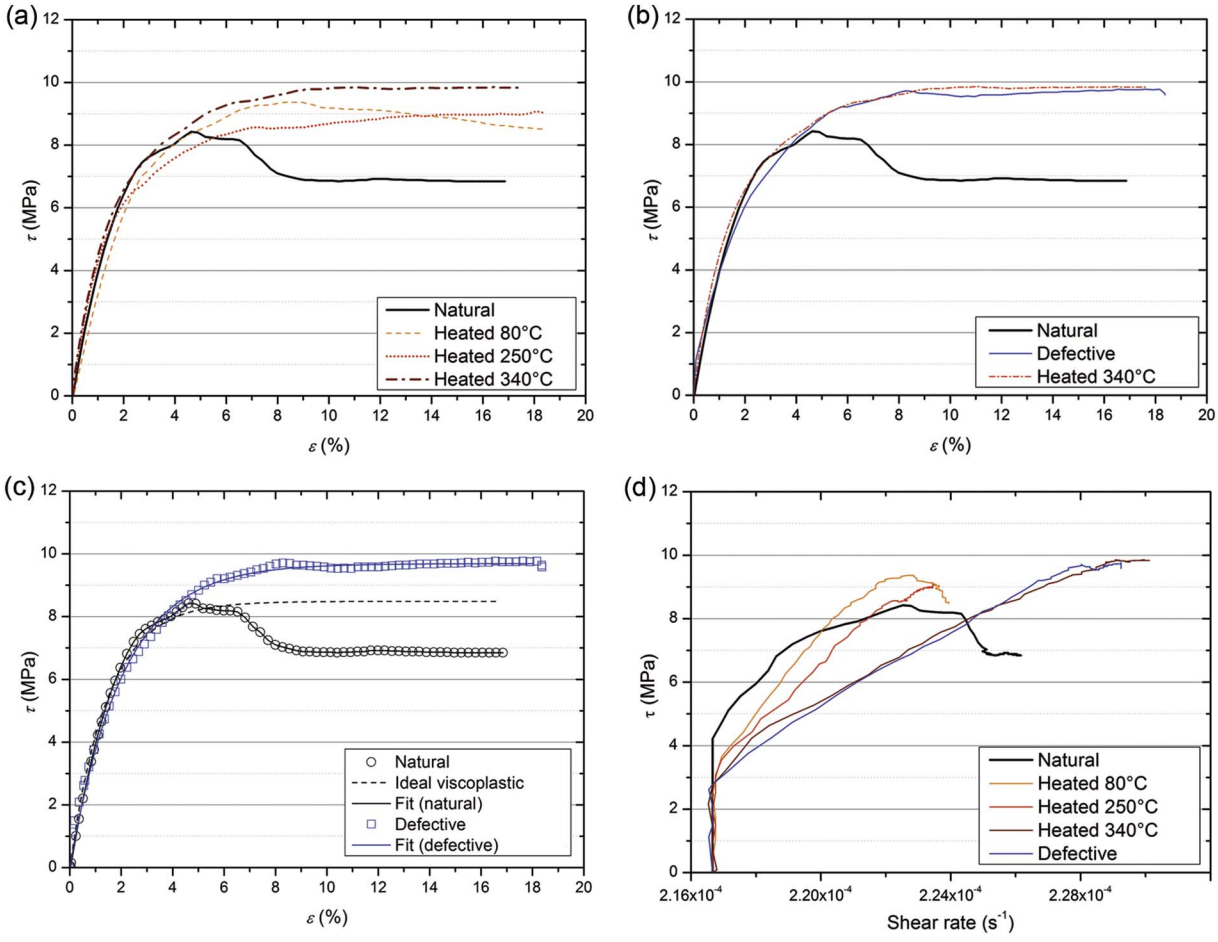

Fig. 6. Comparison of shearing force/deformation curves for (a) natural and heated Ca-montmorillonite and (b) natural, heated up to 340 °C and grinded (defective) Ca-montmorillonite. (c) Fit of the natural and grinded (defective) montmorillonite samples stress/strain curves by the Maxwell model (see text for details). (d) Shear rate/shear stress plot for natural, heated and grinded (defective) Ca-montmorillonite samples.

Table 2
Mechanical parameters for natural, heated and grinded (defective) Ca-montmorillonite obtained from the Mohr-Coulomb criterion.

Sample	Peak shear strength		Residual shear stress	
	ϕ_p (°)	c_p (MPa)	ϕ_r (°)	c_r (MPa)
(1) Natural sample	17.8	1.83	15.6	0.63
(2) Heated up to 80 °C	26.7	0	25.3	0
(3) Heated up to 250 °C	25.8	0	–	–
(4) Heated up to 340 °C	26.9	0	–	–
(5) Grinded, defective sample	27.7	0	26.4	0

montmorillonite has to be explained only in terms of the physical, structural and defective characteristics of individual clay particles. The arrangement and presence of water in the sample has also an important effect.

Natural montmorillonite, containing about 5 wt% of adsorbed water, presenting layer integrity and capability to retain and release water molecules, can be deformed through a sliding mechanism of the clay platelets involving the adsorbed water. It is not possible to exclude the delamination of the 00 *l* planes of the TOT layers (involving interlayer water) that may also occur during the shear test. The former sliding mechanism of the clay platelets results in material compaction and onset of discrete shear planes development, as well displayed by SEM data. A preferred orientation of clay platelets could occur when the failure of materials takes place and the sliding of platelets leads to the development of shear planes, as already observed by Morgenstern and Tchalenko (1967). The material shows a typical strain softening behaviour (Skempton, 1970) related to the sliding of ordered clay platelets favoured by the adsorbed water.

The obtained data suggests that:

(i) the cohesion, compaction and presence of polished surfaces of the material are related to the water adsorbed on the layer surface, whereas
(ii) the presence of the interlayer water affects mainly the development of striated shear planes.

This hypothesis was confirmed by removing (desorbing) the surficial water (about 5% wt.) by heating the sample at 80 °C and performing the same shear test, obtaining only scaly cleavage and striations and no polished surfaces. Indeed, in the present work it was observed that water was released during the shear test only from the starting natural sample. Consequently, the softening and pseudo-plastic behaviour of Ca-montmorillonite has to be attributed to the absorbed water and sliding of ordered clay platelets. Furthermore, the sample heated at 80 °C, which mainly lost the adsorbed water, still presents a shear softening behaviour (even if of reduced entity respect the starting material), showing through optical microscopy and SEM striated surfaces. This behaviour seems to be related to the presence of the interlayer water.

Samples heated up to 250 and 340 °C, which respectively have partially and completely lost the interlayer water molecules (about 3% wt.), do not show neither development of scaly cleavage nor striations on the principal shear surface. They show a more plastic behaviour, because the lack of both adsorbed and interlayer water hinders the sliding mechanisms of clay particles and thus the development of secondary shear planes, as indicated also by Skempton (1966) and Morgenstern and Tchalenko (1967). These observations are in agreement with the proposed mechanical modelling, which describes in an adequate way the observed mechanical shear behaviour of Ca-montmorillonite. The strain softening function $h(\varepsilon)$ and the viscosity of the material is strongly related to the type of water molecules in the samples and the heating/grinding treatments.

The shear behaviour of the grinded (ball-milled) Ca-montmorillonite confirms this hypothesis. In this case, the clay contains both adsorbed and interlayer water, but presents defective and damaged TOT layers. The montmorillonite does not release water under the shear test, and presenting a severe lack of ordering and a partial destruction of the clay platelets (Dellisanti and Valdrè, 2005), is hindered to a deformation by a sliding mechanism and therefore to a rearrangement and alignment of the clay platelets. In addition, since the defective structure has lost the capability to absorb and release water, it shows only plastic behaviour.

The results of the present research seem to indicate the extremely important role played by the different kind of water molecules (surface and interlayer) and, concomitantly, by the ordering and the integrity of the clay platelets on the $\tau(\varepsilon)$ and $\tau(\dot{\varepsilon})$ shear mechanical behaviour of Ca-montmorillonites. These interesting results may find useful applications in technology and industrial use of montmorillonites and other phyllosilicates where both grinding and water treatment are required.

References

Ahlgren, S.G., 2001. The nucleation and evolution of Riedel shear zone as deformation bands in porous sandstone. J. Struct. Geol. 23, 1203–1214.

Bandara, W., Krishantha, D.M.M., Perera, J., Rajapakse, R.M.G., Tennakoon, D.T.B., 2005. Preparation, characterization and conducting properties of nanocomposites of successively intercalated polyaniline (PANI) in montmorillonite (MMT). J. Compos. Mater. 39, 759–775.

Bennet, R.H., Bryant, W.R., Keller, G.H., 1981. Clay fabric of selected submarine sediments: fundamental properties and models. J. Sediment. Petrol. 51, 217–232.

Bennet, R.H., Bryant, W.R., Hulbert, M.H., 1991. Determinants of clay and shale microfabric signatures: processes and mechanisms. In: Bennet, R.H., Bryant, W.R., Hulbert, M.H. (Eds.), Microstructure of Fine-grained Sediments. From Mud to Shale. Springer-Verlag, pp. 5–32 (1991).

Cao, Z.F., Xia, Y.Q., Xi, X., 2017. Nano-montmorillonite-doped lubricating grease exhibiting excellent insulating and tribological properties. Friction 5, 219–230.

Casagrande, A., 1932. The Structure of Clay and Its Importance in Foundation Engineering. Amer. Soc. Of Civil Engin, Boston.

Chandler, R.J., 1984. Recent European experience of landslides in overconsolidated clay and soft rocks. In: Proceedings Iv Int. Symposium ON Landslides Toronto. vol. 1. pp. 61–81.

Christidis, G.E., Makri, P., Perdikatsis, V., 2004. Influence of grinding on the structure and colour properties of talc, bentonite and calcite white fillers. Clay Miner. 39, 163–175.

Christidis, G.E., Dellisanti, F., Valdrè, G., Makri, P., 2005. Structural modifications of smectites mechanically deformed under controlled conditions. Clay Miner. 40, 511–522.

Dellisanti, F., 2004. Relazioni tra deformazioni di taglio e caratteri minero-petrografici di peliti nell'Appennino Settentrionale. PhD Thesis. Università di Bologna, Italy, pp. 104.

Dellisanti, F., Valdrè, G., 2005. Study of structural of ion treated and mechanically deformed commercial bentonite. Appl. Clay Sci. 28, 233–244.

Dellisanti, F., Minguzzi, V., Valdrè, G., 2006. Thermal and structural properties of Ca-rich montmorillonite mechanically deformed by compaction and shear. Appl. Clay Sci. 31, 282–289.

Dellisanti, F., Pini, G.A., Tateo, F., Baudin, F., 2008. The role of tectonic shear strain on the evaluation of illite "crystallinity" parameters. A case study from a fault zone in the northern Apennines, Italy. Int. J. Earth Sci. 97, 601–616.

Dong, X.Q., Wang, L., Yang, X.H., Lin, Y.X., Xue, Y.Z., 2015. Effect of ester based lubricant SMJH-1 on the lubricity properties of water based drilling fluid. J. Pet. Sci. Eng. 135, 161–167.

Filipović-Petrović, L., Kostic-Gvozdenovic, L., Eric-Antonic, S., 2002. The effects of the fine grinding on the physicochemical properties and thermal behaviour of bentonite clay. J. Serbian Chem. Soc. 67 (11), 753–760.

Hight, D.W., El Ghamrawy, M.K., Gens, A., 1979. Some results from a laboratory study of a sandy clay and implications regarding its in-situ behaviour. In: Proceedings of the 2nd International Conference on the Behaviour of Off-shore Structures. vol. 1. pp. 133–150.

Krumm, S., 1996. WINFIT 1.0 – a computer program for X-ray diffraction line profile analysis. Acta Univ. Carol. Geol. 38, 253–261.

Lupini, J.F., Skinner, A.E., Vaughan, P.R., 1981. The drained residual strength of cohesive soils. Geotechnique 31 (2), 181–213.

Menesi, J., Korosi, L., Bazso, E., Zollmer, V., Richardt, A., Dekany, I., 2008. Photocatalytic oxidation of organic pollutants on titania-clay composites. Chemosphere 70, 538–542.

Morgenstern, N.R., Tchalenko, J.S., 1967. Microscopic structures in kaolin subjected to direct shear. Geotechnique 17 (4), 309–328.

Müller, B.U., Schlüchter, C., 2001. Influence of the glacier bed lithology on the formation of a subglacial till sequence – ring-shear experiments as a tool for the classification of subglacial tills. Quat. Sci. Rev. 20, 1113–1125.

Müller-Vonmoos, M., Honold, P., Kahr, G., 1985. Des Scherverhalten reiner Tone. Mitteilungen des Instituts für Grundbau und Boden-mechanik. vol. 122. ETH-Zürich, pp. 3–22.

Novak, I., Čičel, B., Jakubekova, D., 1982. Changes in the texture of bentonite occurring

during vibration grinding and after aging. Silikàty 26, 15–20.
Olson, R.E., 1974. Shearing strength of kaolinite, illite and montmorillonite. J. Geotech. Eng. Div. 100, 1215–1299.
Pini, G.A., 1999. Tectonosomes and Olistostromes in the Argille Scagliose of the Northern Apennines, Italy. The Geological Society of America, pp. 70 Special Paper 335.
Skempton, A.W., 1964. Long term stability of clay slopes. Geotechnique 14 (2), 77–101.
Skempton, A.W., 1966. Some observation of tectonic shear zones. In: Proceedings, International Society of Rock Mechanics Congress, 1st ed. 6. International Society of Rock Mechanics, Lisbon, pp. 329–335.
Skempton, A.W., 1970. First-time slides in over-consolidated clays. Geotchnique 20 (3), 320–324.
Skinner, A.E., 1969. A note on the influence of inter-particle friction on the shearing strength of a random assembly of spherical particles. Geotechnique 19, 150–157.
Tchalencko, J.S., 1968. The evolution of kink-bands and the development of compression textures in sheared clay. Tectonophysics 6, 159–174.
Tchalencko, J.S., 1970. Similarities between shear zones of different magnitudes. Geol. Soc. Am. Bull. 81, 1625–1640.
Terzaghi, K., 1936. The shear resistance of saturated soils. In: Proc. First International Conference on Soil Mechanics & Foundation Engineering, Cambridge, MA. vol. 1. pp. 54–56.
Vannucchi, P., Maltman, A., Bettelli, G., Clennell, B., 2003. On the nature of scaly fabric and scaly clay. J. Struct. Geol. 25 (5), 673–688.
Vaughan, P.R., Davachi, M.M., El Ghamrawy, M.K., Hamza, M.M., Hight, D.W., 1976. Stability analysis of large gravity structures. In: Proceedings of the 1st International Conference on the Behaviour of Off-shore Structures. vol. 1. pp. 467–480.
Volzone, C., Aglietti, E.F., Scian, A.N., Porto Lopez, J.M., 1987. Effect of induced structural modifications on the physicochemical behaviour of bentonite. Appl. Clay Sci. 2, 97–104.
Wu, X.W., Wu, N., Shi, C.Q., Zheng, Z.Y., Qi, H.B., Wang, Y.F., 2016. Proton conductive montmorillonite-Nafion composite membranes for direct ethanol fuel cells. Appl. Surf. Sci. 388, 239–244.
Yong, R.N.A., McKyes, E., 1971. Failure and yield of a clay under triaxial stresses. J. Soil Mech. Found. Div. 97, 159–176.